Drug Development and Industrial Pharmacy, 34:1022–1035, 2008

ISSN: 0363-9045 print / 1520-5762 online
DOI: 10.1080/03639040801925990

informa
healthcare

Utility of Multivariate Analysis in Modeling the Effects of Raw Material Properties and Operating Parameters on Granule and Ribbon Properties Prepared in Roller Compaction

Josephine L. P. Soh, Feng Wang, Nathan Boersen, Rodolfo Pinal, Garnet E. Peck, and M. Teresa Carvajal
Department of Industrial and Physical Pharmacy, School of Pharmacy and Pharmaceutical Sciences, Purdue University,West Lafayette, IN, USA

James Cheney, Hedinn Valthorsson, and Jim Pazdan
Global Process Analytical Technology, Novartis Pharmaceuticals Corporation, Suffern, New York, USA

This article aimed to model the effects of raw material properties and roller compactor operating parameters (OPs) on the properties of roller compacted ribbons and granules with the aid of principal component analysis (PCA) and partial least squares (PLS) projection. A database of raw material properties was established through extensive physical and mechanical characterization of several microcrystalline cellulose (MCC) and lactose grades and their blends. A design of experiment (DoE) was used for ribbon production. PLS models constructed with only OP-modeled roller compaction (RC) responded poorly. Inclusion of raw material properties markedly improved the goodness of fit (R^2 = .897) and model predictability (Q^2 = 0.72).

Keywords roller compaction; near-infrared spectroscopy; material characterization; microcrystalline cellulose; multivariate data analysis; process analytical technology

INTRODUCTION

Roller compaction (RC) is a continuous dry granulation process that involves the densification of powder between two counter-rotating rolls. The ribbons formed are then milled into granules of desired particle size, size distribution, and flow and bulk density for tableting and capsule filling (Cohn, Heilig, & Delorimier, 1966; Hariharan, Wowchuk, Nkansah, & Gupta, 2004; Inghelbrecht & Remon, 1998a). RC is a relatively uncomplicated and inexpensive process that offers distinct advantages over wet granulation particularly for moisture-, solvent-, or heat-sensitive compounds. In the pharmaceutical industry, RC is an attractive option for considerable cost savings because of high production throughput, elimination of drying step that reduces production, and development time as well as ease of scale-up (Inghelbrecht & Remon, 1998b).

Although RC has been utilized in the manufacturing of a variety of products, there is currently no well-established "quality-by-design" methodology to include raw material variation in the efficient operation of the roller compactor. Thus, RC formulation and process development still rely largely on experience, trial-and-error, and empirical design of experiment (DoE) though some researchers have begun to model the process (Johanson, 1965; Simon & Guigon, 2003; Turkoglu, Aydin, Murray, & Sakr, 1999), including newer attempts using finite element modeling (Dec, Zavaliangos, & Cunningham, 2003). The latter method was concluded to be the most versatile approach because it incorporates information pertaining to powder behavior, geometry, and frictional interactions (Dec et al., 2003).

With the launch of the process analytical technology (PAT) initiative by the U.S. Food and Drug Administration in 2004, there has been a commensurate increase in the use of analytical techniques, especially near-infrared spectroscopy (NIR) for on-, in-, and at-line measurements. These measurements of critical quality and performance attributes of raw materials, in-process materials, and processes provide timely control and feedback, which in turn ensure end-product quality (Gupta, Miller, & Morris, 2005a). Gupta, Miller, and Morris, (2004, 2005b, 2005c) had also established the usefulness of NIR as a robust process control tool to predict ribbon attributes, monitor and control manufacturing processes in RC. Figure 1 shows the schematic diagram for process monitoring and feedback control of RC using NIR.

Apart from RC operating parameters (OPs), variations in raw material properties also play a significant role in governing

Address correspondence to M. Teresa Carvajal, IPPH, Purdue University, 575 Stadium Mall Drive, West Lafayette, IN 47907. E-mail: carvajal@pharmacy.purdue.edu

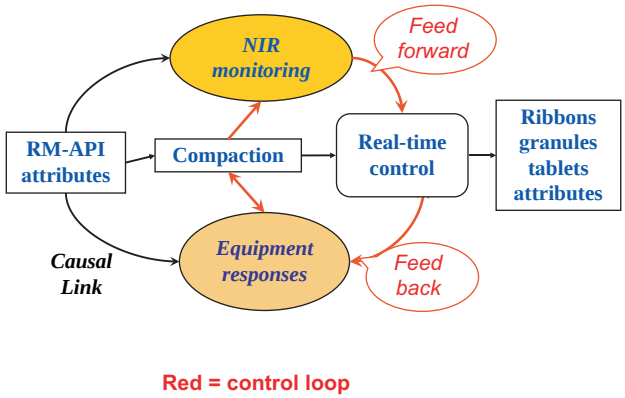

FIGURE 1. Schematic diagram for process monitoring and control of roller compaction.

the resultant ribbon and granule characteristics. Consequently, a good understanding on how various raw material attributes affect ribbon and granule properties is crucial during formulation, optimization, and process control. In particular, the ability to identify critical raw material attributes and assess their relative influence in end-product quality will be especially advantageous.

Hence, the main objective of this article was to identify the critical material attributes that govern the ribbon and granule properties with the aid of multivariate data analysis. Microcrystalline cellulose (MCC) and lactose are commonly used to represent plastically deforming and brittle fracturing materials, respectively, in dry granulation and tableting. Hence, three grades of each material were used to provide a range of raw material properties. The first step involved extensive material characterization to establish a comprehensive database of their physical and mechanical attributes. Ribbons were then prepared according to a DoE that included a 2^3 full factorial design. Together with the OP, the effects of these raw material properties on the ribbon, granule, and RC responses were modeled using principal component analysis (PCA) and partial least squares (PLS) regression. From the results obtained, it was possible to see the effects of raw material properties on the overall predictability of end-product quality as well as to identify the OP and raw material properties that exerted dominant influences on ribbon and granule properties.

MATERIALS AND METHODS

Materials

Three grades of MCC and three grades of lactose (two monohydrate and one anhydrous) were used in this study. The MCC grades were Emcocel 50M, Emcocel 90M, and Emcocel SCG (J.R.S. Pharma LP, NY, USA). Emcocel SCG was an MCC grade that was customized and specially manufactured for Novartis Pharmaceuticals Corporation (Suffern, NY, USA). The two lactose monohydrate grades were Monohydrate Regular (Foremost Farms, WI, USA) and Pharmatose 200M (DMV International, Veghel, the Netherlands). The anhydrous lactose grade was Lactose DT (Kerry Bio-Science, NY, USA). Magnesium stearate (MgSt) (Mineral and Pigment Solutions, Inc., NJ, USA) and colloidal silicon dioxide (SiO_2) (Aerosil; Degussa Corporation, Parsippany, NJ, USA) were the lubricant and glidant, respectively. A total of 21 different formulations were used in this study, and their respective formulae are summarized in Table 1.

Methods

Powder blends were first premixed by geometric dilution mixing in a polyethylene bag before mechanical blending in a bin blender (Model 060064; Tote Systems, Burleson, TX, USA) at 16 rpm for 10 min. The mixed blends were collected and used for the subsequent analyses.

Physical Characterization of Excipients and Powder Blends

Physical and mechanical characteristics of the excipients and their respective powder blends were systematically classified under five subgroups. They were as follows: (a) MCC weight fraction (wt/wt) and raw material tablet properties, (b) compressibility indices, (c) bulk density, (d) particle size, and (e) powder flow properties. The MCC fraction was calculated as the mass of MCC relative to the total mass of MCC and lactose excluding glidant and lubricant, which were both fixed at 2% wt/wt.

Raw Material Tablet Properties

Tablets were prepared from 400 mg of powder using a Carver press (Model 21900–359; Carver Laboratory Press, Fred S. Carver Inc., Summit, NJ, USA), fitted with a 7/16 in. flat-faced punch at a compression force of 3,000 lbs. Twenty tablets were punched for each batch of powder blend and crushed using a Tablet Hardness Tester (VK 200 Tablet Hardness Tester, Model 40–2000; Vankel from Varian Industries Inc., Lake Forest, CA, USA). Tablet tensile strength was calculated from the Brazilian test erroneously called the crushing strength using the following equation.

$$\text{Tensile strength}\,(\sigma_t) = \frac{2F}{\pi Dt}, \tag{1}$$

where F is the crushing strength, D refers to the tablet diameter, and t refers to the tablet thickness.

The tablet solid fraction is defined as the ratio of tablet apparent density to the tablet true density. The tablet apparent density is obtained from the ratio of tablet mass to tablet volume (calculated based on the volume of a cylinder), whereas the tablet true densities of the blends were computed as defined subsequently in Equation 6.

TABLE 1
Formulations for All Batches Used in this Study

Batch Number	MCC/Lactose	Amount (%wt/wt)	SiO_2 (%wt/wt)	MgSt (%wt/wt)
1	Emcocel 50M	96	2	2
2	Emcocel 90M	96	2	2
3	Emcocel SCG	96	2	2
4	Anhydrous DT	96	2	2
5	Monohydrate	96	2	2
6	Pharmatose 200M	96	2	2
Batch Number	Emcocel SCG (%wt/wt)	Pharmatose 200M (%wt/wt)	SiO_2 (%wt/wt)	MgSt (%wt/wt)
7	0	96	2	2
8	24	72	2	2
9	48	48	2	2
10	72	24	2	2
11	96	0	2	2
Batch Number	Emcocel SCG (%wt/wt)	Lactose DT (%wt/wt)	SiO_2 (%wt/wt)	MgSt (%wt/wt)
12	0	96	2	2
13	24	72	2	2
14	48	48	2	2
15	72	24	2	2
16	96	0	2	2
Batch Number	Emcocel 50M (%w/w)	Pharmatose 200M (%wt/wt)	SiO_2 (%wt/wt)	MgSt (%wt/wt)
17	0	96	2	2
18	24	72	2	2
19	48	48	2	2
20	72	24	2	2
21	96	0	2	2

Compressibility Studies

A Vanderkamp Tap Density Tester (Model 10705; Vankel Industries Inc.) was used as a surrogate for compressibility. Powders were poured into a glass funnel supported on a ring stand and positioned above the mouth of a 100-mL measuring cylinder. The powder flowed through the glass funnel to loosely fill the weight-tarred measuring cylinder to the 100 mL graduation. Initial and final weights and volumes occupied by the powders were recorded. Tapping was performed in a 2^n geometric progression, up to 2,048 taps when no further change in volume was observed. Bulk (ρ_b) and tapped densities (ρ_t) were calculated as quotients of the weight of powder to the volumes occupied before and after tapping. Carr indices, Hausner ratios, and Kawakita constants (a and $1/b$) were subsequently derived according to the methods described previously (Carr, 1965; Hausner, 1967; Ludde & Kawakita, 1967). Flowability is characterized as excellent when the Carr index = 5–10, good between 2 and 16, fair when Carr index = 18–21, and poor between 23 and 28. Similar criteria exist for the Hausner ratio. Triplicates were obtained for all and results averaged.

$$\text{Carr index} = \frac{\rho_t - \rho_b}{\rho_t} \tag{2}$$

$$\text{Hausne ratio} = \frac{r_t}{r_b} \tag{3}$$

$$\frac{N}{C} = \frac{1}{ab} + \frac{N}{a}, \tag{4}$$

where N was the number of taps, C was the degree of volume reduction and calculated as

$$C = \frac{V_o - V_n}{V_o}, \tag{5}$$

where V_o was the initial volume and V_n was the bulk volume of the powder after N taps. The constants, a and $1/b$, were related to compressibility and cohesion, respectively.

True Density Determination

True densities of the pure excipients (three MCC grades, three lactose grades, MgSt, and SiO_2) were determined using a helium pycnometer (Micromeritics AccuPyc 1330; Micromeritics, Norcross, GA, USA). MCC and lactose powders were predried in a convection oven at 105°C for 4 h and 50°C overnight, respectively. The dried powders were placed in glass vial bottles and cooled in a desiccator under vacuum before use. Depending on the bulk density of the powders, approximately 3–5 g of powders were used for each analysis. True density analysis was performed in triplicates and results averaged.

From the true densities of the individual excipients, true densities of the respective powder blends were calculated as follows:

$$\begin{aligned}\text{Apparent true density of blend} = {} & a \times \text{true density (MCC)} + b \times \\ & \text{true density (lactose)} + c \times \\ & \text{true density (MgSt)} + \\ & d \times \text{true density } (SiO_2)\end{aligned} \quad (6)$$

where *a*, *b*, *c*, and *d* are the weight proportion of MCC, lactose, MgSt, and SiO_2 stipulated in the respective batches.

Particle Size Determination

Particle size was determined by laser diffraction (Helos; Sympatec Inc., Pulverhaus, Germany). All powders were presieved with a 425-μm aperture size sieve before size analysis. Powders were steadily delivered using a dry powder dispersion module (RODOS; Sympatec Inc.) that uses positive air pressures (of up to 6 bars) to disperse the powders. Inlet air pressures ranged from 1 to 1.3 bars for effective dispersion of the powders used in this study. A 5-mW He–Ne laser (wavelength = 632.8 nm) was used for particle sizing. Eight interchangeable measurement ranges (R1–R8) are available on this laser diffraction system, depending on the size of the particles measured. Apart from batches 12–16 that were measured using the R5 range (0–875 μm), particle size analysis of the other powders was performed at the R4 measuring range (0–350 μm). Batches 12–16 were composed of Emcocel SCG and Lactose DT, whose particle sizes were larger than the measurable range provided by R4.

Their (volume weighted) mean particle diameter was automatically determined while particle size distribution was represented by span and calculated as follows. Five repeats were carried out.

$$\text{Span} = \frac{X_{90} - X_{10}}{X_{50}} \quad (7)$$

where X_{10}, X_{50}, and X_{90} were the diameters of powder particles at the 10, 50, and 90 percentiles of the cumulative percent undersize plot, respectively.

Powder Flow Properties

Angles of repose and fall were measured using a Hosokawa powder tester (Hosokawa Micron, Osaka, Japan). An aliquot of powder was accurately weighed out for every batch and poured into a glass funnel. The powder flowed through the glass funnel onto a 710-μm aperture size sieve which was vibrated at an amplitude of 1 mm. The sieved powder was directed from another glass funnel to form a heap on the stainless steel stand positioned underneath it. The amount of powder varied between the batches and was estimated to be the amount required to form a powder heap and overfill the stainless steel stand below. Replicate readings for the same batch were taken using the same amount of powders.

The angle formed between the side of the heap and the horizontal is defined as the repose angle. Three controlled mechanical shocks were applied to the stationary powder mass, causing it to collapse. The new angle formed between the side of the new heap and the horizontal is known as the angle of fall. Four readings were obtained for both angles of repose and fall and results averaged. The difference between the angle of repose and the angle of fall was known as the angle of difference. The angles of both fall and difference could be used to indicate powder floodability.

Roller Compaction

Compacts were prepared on a pilot scale roller compactor (IR-520; The Fitzpatrick Company, Elmhurst, IL, USA) using the formulations listed in Table 1. The ranges of roller compactor OPs are as follows:

- Roll speed (6–22 rpm)
- Roll gap (0.02–0.25 in.)
- Roll pressure (0–1,600 psi)
- Vertical feed screw (VFS) speed (50–350 rpm)
- Horizontal feed screw (HFS) speed (18–109 rpm)
- Mill speed (50–500 rpm).

The VFS speed and mill speed were held constant at 225 and 150 rpm, respectively, in all the experiments performed. As part of the preliminary studies to establish the operating range of the roller compactor, batches 1–6 were used to prepare ribbons at the conditions stated in Table 2. The production capacity of the Fitzpatrick IR-520 is 0.165–1.65 kg/min. In this study, a mass flow rate of around 1.0 kg/min was used, depending on the HFS speed. For each run, the compactor was given approximately 1 min to reach steady state before actual sample collection and data recording in the next 3 min.

In the preliminary experiments (batches 1–6), only lubricated MCC or lactose was compacted. To simulate more realistic formulations (i.e., combinations of elastic and plastically deforming materials), 15 other formulations containing a mixture of lactose and MCC in varying proportion were used for ribbon production. A 2^3 full factorial design with two axial points in the roll pressure direction and two replicates of center

TABLE 2
Operating Levels for Screening and Design of Experiment (DoE) Study

Batch Number	Roll Speed (rpm)	HFS Speed (rpm)	Roll Pressure (rpm)
1–6 (screening)	12	40	300
	9	60	300
	15	20	300
	15	60	300
7–21 (DoE)			
Factorial	8	35	400
	8	65	400
	8	35	600
	8	65	600
	14	35	400
	14	65	400
	14	35	600
	14	65	600
Center	11	50	500
	11	50	500
	11	50	500
Axial	11	50	350
	11	50	650

point (total of 13 runs per formulation) was used for the remaining controllable factors (roll speed, roll pressure, and HFS speed) and shown in Table 2. In this study, it was of interest to understand the effects of raw material properties on roll gap that can be used as a process critical control parameter (PCCP). For this reason, the roll gap was treated as a response factor rather than an OP here.

Characterization of Compacts

Compacts were characterized by their apparent density (Rib_dens), relative density (defined below), and NIR slope. The ribbon relative density is positively correlated to the mechanical strength of the ribbon. The apparent ribbon density is defined by the equation:

$$\rho_{app} = \frac{m_r}{V_r}, \tag{8}$$

where m_r and V_r refer to the ribbon mass and volume, respectively. The ribbon volume V_r was determined from the measurement of the ribbon dimensions.

The ribbon relative density is the ratio of the apparent to the true density. The true density, which is uniquely determined by the nature of the powders constituting the blend, needs to be determined from the raw material alone. The ribbon relative density was correlated to the slope of its NIR spectrum. This procedure involves the irradiation of the ribbon with infrared light in the wavelength range of 1,093–2,212 nm. During the measurement, the frequencies corresponding to the resonant frequencies of the molecules constituting the ribbons are absorbed. The NIR slope is determined by fitting the resulting spectrum to a straight line. The setup for NIR monitoring of the RC process is shown in Figure 2.

Characterization of Granules and Tablets

Prepared compacts were milled and the granules collected were sized and tableted. Particle size of granules was determined by sieving the granules collected from the mill through a nest of U.S. Standard Test Sieves (W.S. Tyler, Mentor, Ohio, USA) whose aperture sizes ranged from 45 to 1,400 μm. The granule mean particle size (GMPS) was the 50th percentile of the cumulative percent oversize plot. Tablets were also prepared from these granules in a similar way as those prepared from the powder blends except that a different model of Carver press and punch (no. 486 flat-faced punch) was used in the preparation of these tablets (Model C; Carver Laboratory Press, Fred S. Carver Inc.). The tensile strength of tablets prepared from granules Granule tablets tensile strength (GTTS) was determined using a tablet tester (Model 6D; Dr. Schleuniger, Pharmatron AG, Solothurn, Switzerland) and calculated as per Equation 1.

Multivariate Data Analysis

PCA and PLS regression were performed using the multivariate data analysis algorithms in the SIMCA software package (SIMCA P+, version 11; Umetrics Academy, Malmö, Sweden). All variables were scaled to unit variance (UV) before analysis.

RESULTS AND DISCUSSION

Physical Properties of Pure Excipients and Their Respective Blends

Selected physical properties of the pure excipients are summarized in Table 3. Generally, the best compressibility was observed in the two coarse MCC grades, Emcocel 90M and Emcocel SCG, whereas Pharmatose 200M had the poorest compressibility. This is because of the small particle size and high cohesiveness within the bulk powder mass of Pharmatose 200M.

Physical properties of the 21 batches of powder blends are summarized in Tables 4 and 5. RM_TTS increased with increasing MCC fraction (batches 7 through 11, batches 12 through 16, and batches 17 through 21). The strongest tablets were prepared with Emcocel 50M (batches 1 and 21), and this was attributed to the small particle size of this MCC grade that increased the surface area available for stronger interparticulate bonding. Significant improvement in powder compressibility (Table 4) was observed when the MCC grade was changed from Emcocel 50M (batch 21) to Emcocel SCG (batch 11).

Powder flow properties for the pure excipients (in the presence of SiO_2 and Mgst) as well as that for selected powder

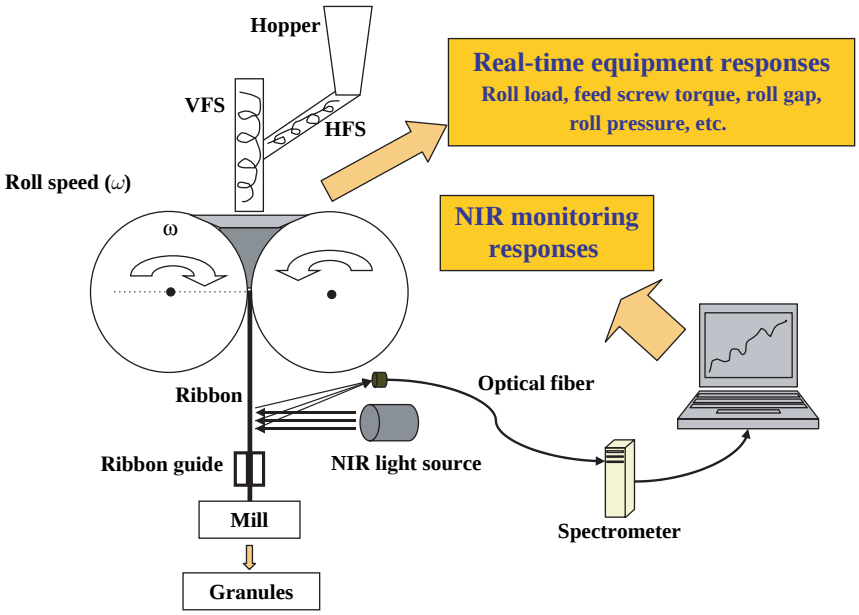

FIGURE 2. Setup for near-infrared (NIR) monitoring of roller compaction (RC) process.

TABLE 3
Physical Properties of Raw Materials Used in this Study (mean ± *SD*)

Property	Monohydrate Regular	Pharmatose 200M	Lactose DT	Emcocel 50M	Emcocel 90M HD	Emcocel 90M SCG
Carr index	37.0 ± 1.7	41.0 ± 1.0	29.7 ± 0.3	28.7 ± 0.8	19.8 ± 1.0	19.8 ± 1.0
Hausner ratio	1.59 ± 0.04	1.70 ± 0.03	1.42 ± 0.01	1.40 ± 0.02	1.25 ± 0.02	1.25 ± 0.02
A	0.38 ± 0.02	0.42 ± 0.01	0.30 ± 0.00	0.29 ± 0.01	0.20 ± 0.01	0.27 ± 0.11
1/*b*	27.5 ± 7.2	34.4 ± 2.9	13.2 ± 0.7	21.0 ± 3.1	11.7 ± 2.2	15.2 ± 4.8
True density (g/mL)	1.49 ± 0.02	1.47 ± 0.02	1.51 ± 0.02	1.47 ± 0.03	1.43 ± 0.01	1.46 ± 0.03
Bulk density (g/mL)	0.62 ± 0.01	0.51 ± 0.00	0.58 ± 0.01	0.33 ± 0.00	0.34 ± 0.00	0.32 ± 0.00
Tapped density (g/mL)	0.99 ± 0.01	0.87 ± 0.01	0.83 ± 0.01	0.46 ± 0.00	0.43 ± 0.00	0.47 ± 0.00
Particle size (μm)	72.57 ± 0.32	40.10 ± 1.14	166.97 ± 4.86	40	82	90
Span	2.77 ± 0.00	3.06 ± 0.04	2.17 ± 0.01	–	–	–

Particle size data of MCC grades were obtained from the manufacturer's specifications.

blends are summarized in Table 5. Generally, Emcocel 90M, Emcocel SCG, and anhydrous lactose (Lactose DT) flowed better than the remaining three excipients, and this was attributed to their larger particle size (Table 3). For powder blends, batches 12–16 that were composed of anhydrous lactose and Emcocel SCG gave the most favorable flow (Table 5). This was not unexpected because the flow properties of these two excipients were the best amongst all six excipients studied.

Influence of OPs on RC Responses for Preliminary Runs

The range of RC responses obtained in the preliminary runs for batches 1–6 are summarized in Table 6. As a representative example of the preliminary runs, batch 3 is used here to study the influences of roller compactor parameters and their optimal ranges for different raw materials (Table 7). VFS and mill speed were kept constant and excluded from analysis. Because roll gap is controlled to maintain other operational parameters at set points, roll gap was regarded as a response. Thus, there were a total of 11 variables in all, 3 factors and 8 responses.

PCA results for batch 3 yielded a one-component model with explained variation (R^2X) of 0.671 and the predicted variation (Q^2) of 0.467. From Figure 3, it was clear that neither Carr index or roll gap were well modeled. Subsequently, the three factors with their respective cross terms were used to formulate the data matrix for PLS analysis. With four components, the cumulative explained variation for the *X*-variables and *Y*-variables were 0.667 and 0.966, respectively, while the

TABLE 4
Physical Properties (Group A and B) of Powder Blends for Batches 1–21 (Mean ± *SD*)

	Group A			Group B			
Batch Number	MCC Fraction	RM_SF	RM_TTS (MPa)	Carr Index (%)	Hausner Ratio	*a*	1/*b*
1	0.96	0.83 ± 0.01	3.78 ± 0.30	32.3 ± 0.9	1.48 ± 0.02	0.32 ± 0.01	22.9 ± 1.2
2	0.96	0.82 ± 0.01	3.63 ± 0.11	30.7 ± 2.1	1.44 ± 0.04	0.31 ± 0.02	17.6 ± 3.3
3	0.96	0.81 ± 0.01	3.26 ± 0.14	25.5 ± 1.3	1.34 ± 0.02	0.26 ± 0.01	15.6 ± 1.9
4	0	0.79 ± 0.01	1.34 ± 0.14	27.2 ± 0.6	1.37 ± 0.01	0.27 ± 0.01	21.7 ± 1.4
5	0	0.82 ± 0.01	0.72 ± 0.09	33.3 ± 1.3	1.50 ± 0.03	0.34 ± 0.01	40.9 ± 2.4
6	0	0.81 ± 0.01	0.78 ± 0.10	38.8 ± 1.3	1.64 ± 0.03	0.39 ± 0.01	53.7 ± 1.2
7	0	0.81 ± 0.01	0.78 ± 0.10	38.8 ± 1.3	1.64 ± 0.03	0.39 ± 0.01	53.7 ± 1.2
8	0.24	0.81 ± 0.01	1.12 ± 0.08	37.3 ± 0.8	1.60 ± 0.02	0.38 ± 0.01	33.7 ± 1.1
9	0.48	0.83 ± 0.01	1.73 ± 0.13	30.3 ± 1.2	1.44 ± 0.02	0.30 ± 0.01	25.9 ± 3.2
10	0.72	0.81 ± 0.01	2.36 ± 0.15	25.8 ± 0.3	1.35 ± 0.01	0.26 ± 0.00	17.9 ± 1.9
11	0.96	0.81 ± 0.01	3.26 ± 0.14	25.5 ± 1.3	1.34 ± 0.02	0.26 ± 0.01	15.6 ± 1.9
12	0	0.79 ± 0.01	1.34 ± 0.14	27.2 ± 0.6	1.37 ± 0.01	0.27 ± 0.01	21.7 ± 1.4
13	0.24	0.82 ± 0.01	1.75 ± 0.14	26.8 ± 0.3	1.37 ± 1.37	0.27 ± 0.27	17.6 ± 3.31
14	0.48	0.82 ± 0.01	2.24 ± 0.08	24.8 ± 0.3	1.33 ± 1.33	0.25 ± 0.25	17.6 ± 3.31
15	0.72	0.82 ± 0.01	2.58 ± 0.14	24.0 ± 1.0	1.32 ± 1.32	0.24 ± 0.24	17.6 ± 3.31
16	0.96	0.84 ± 0.01	3.29 ± 0.11	25.5 ± 1.3	1.34 ± 0.02	0.26 ± 0.01	15.6 ± 1.9
17	0	0.82 ± 0.01	0.76 ± 0.11	38.8 ± 1.3	1.64 ± 0.03	0.39 ± 0.01	53.7 ± 1.2
18	0.24	0.82 ± 0.01	1.34 ± 0.09	37.4 ± 1.0	1.60 ± 0.03	0.41 ± 0.04	43.6 ± 9.3
19	0.48	0.81 ± 0.01	1.89 ± 0.15	36.4 ± 0.0	1.57 ± 0.00	0.37 ± 0.00	34.1 ± 3.9
20	0.72	0.82 ± 0.01	2.74 ± 0.14	33.6 ± 2.5	1.51 ± 0.06	0.34 ± 0.02	24.2 ± 1.3
21	0.96	0.83 ± 0.01	3.78 ± 0.30	32.3 ± 0.9	1.64 ± 0.02	0.32 ± 0.01	22.9 ± 1.2

a and 1/*b* are referred to as kawakita constants.

cumulative predicted variation was 0.495. These values indicated that the predictive ability of the model was poor even though the goodness of fit was acceptable.

From the variable importance in projection (VIP) plot (Figure 4A), it is possible to identify the factors that exerted a stronger influence on the responses by comparing the VIP values. This is similar to comparing the size of coefficients in a linear multiple regression analysis when the factors are all scaled to unit variance. Factors with VIP values larger than 1 are the most important in predicting the *Y*-variables. In this model, roll pressure and roll speed were found to be of major importance in modeling the eight RC responses. Roll pressure was the most dominant factor because of its largest VIP value (Figure 4A). Although the VIP value for roll speed was larger than RS*HFS, RS*RP, HFS, and HFS*RP, these differences were not deemed to be statistically significant because of the uncertainty, that is, the large error bars.

The relative significance of each *X*-variable in the measured responses is also observed in the coefficient overview plot (Figure 4B). The magnitude of the coefficients reflects the degree of influence of that particular factor on a given response, whereas the sign of coefficient dictates the direction of the influence, whether positive or negative. From Figure 4B, it was clear that roll pressure exerted a large, positive effect on most of the responses, such as NIR slope, measured and predicted ribbon density as well as the GMPS. On the contrary, roll speed had a large negative effect on roll gap: the higher the roll speed, the smaller the roll gap as expected.

PLS Regression for Mixed Excipient Batches

Upon completion of the screening experiment, the important factors and their optimal ranges resulting in desired ribbon properties for a given raw material (pure MCC or lactose) were identified. However, the preliminary experiments only involved pure raw materials and therefore provided no information on mixtures of raw materials. In this section, the influence of OPs on binary mixtures of MCC and lactose are evaluated, yielding information about the effects of raw material variation on the properties of the resulting ribbons and granules.

Furthermore, the preliminary experiments were designed chiefly for screening and as such possessed only two levels for each operational parameter and one center point without any replicate. This means that the resulting model included neither nonlinear relationships between factors and responses nor an error estimate. To get a model with better predictability, axial

TABLE 5
Physical Properties (Groups C–E) of Batches 1–21 (Mean ± *SD*)

	Group C			Group D		Group E		
Batch Number	True Density (g/mL)	Bulk Density (mL)	Tapped Density (mL)	Particle Size (μm)	Span	Angle_Repose	Angle_Fall	Angle_Diff
1	1.40 ± 0.03	0.32 ± 0.00	0.47 ± 0.00	62 ± 4.20	2.53 ± 0.08	46.90 ± 2.19	28.18 ± 2.70	18.73 ± 4.30
2	1.44 ± 0.03	0.31 ± 0.01	0.45 ± 0.01	–	–	41.93 ± 0.91	27.05 ± 1.10	14.88 ± 2.00
3	1.43 ± 0.03	0.35 ± 0.00	0.47 ± 0.00	130 ± 3.29	1.93 ± 0.01	44.93 ± 1.24	26.63 ± 2.60	18.30 ± 2.03
4	1.49 ± 0.02	0.57 ± 0.01	0.79 ± 0.01	90 ± 0.21	3.63 ± 0.04	44.6 ± 0.88	32.55 ± 1.30	12.05 ± 2.16
5	1.47 ± 0.02	0.55 ± 0.01	0.82 ± 0.00	–	–	47.85 ± 1.45	35.13 ± 2.76	12.73 ± 4.21
6	1.45 ± 0.02	0.47 ± 0.01	0.76 ± 0.01	36 ± 1.14	4.00 ± 0.06	50.68 ± 0.89	32.25 ± 1.50	18.43 ± 1.41
7	1.45 ± 0.02	0.47 ± 0.01	0.76 ± 0.01	36 ± 1.14	4.00 ± 0.06	50.68 ± 0.89	32.25 ± 1.50	18.43 ± 1.41
8	1.45 ± 0.01	0.46 ± 0.01	0.74 ± 0.00	56 ± 2.83	5.00 ± 0.14	50.10 ± 0.72	26.83 ± 0.68	23.28 ± 0.75
9	1.44 ± 0.00	0.44 ± 0.00	0.64 ± 0.01	74 ± 0.62	4.11 ± 0.03	44.63 ± 0.87	25.68 ± 1.54	18.95 ± 2.29
10	1.44 ± 0.01	0.41 ± 0.00	0.56 ± 0.00	91 ± 0.56	2.82 ± 0.01	42.75 ± 1.49	25.13 ± 0.85	17.63 ± 2.06
11	1.43 ± 0.03	0.35 ± 0.00	0.47 ± 0.00	130 ± 3.29	1.93 ± 0.01	44.93 ± 1.24	26.63 ± 2.60	18.30 ± 2.03
12	1.49 ± 0.02	0.57 ± 0.01	0.79 ± 0.01	90 ± 0.21	3.63 ± 0.04	44.60 ± 0.88	32.55 ± 1.30	12.05 ± 2.16
13	1.48 ± 0.02	0.49 ± 0.01	0.68 ± 0.01	128 ± 3.87	2.61 ± 0.00	43.93 ± 1.88	26.23 ± 1.27	17.70 ± 3.07
14	1.46 ± 0.01	0.44 ± 0.01	0.59 ± 0.01	97 ± 0.37	2.33 ± 0.04	44.65 ± 1.21	26.40 ± 1.25	18.25 ± 2.03
15	1.45 ± 0.02	0.40 ± 0.01	0.52 ± 0.01	129 ± 5.02	2.09 ± 0.05	42.35 ± 0.54	25.40 ± 0.85	16.95 ± 0.62
16	1.43 ± 0.03	0.35 ± 0.00	0.47 ± 0.00	130 ± 4.29	1.99 ± 0.02	43.43 ± 0.51	27.23 ± 2.03	16.20 ± 2.49
17	1.45 ± 0.02	0.47 ± 0.01	0.76 ± 0.01	41 ± 2.95	4.19 ± 0.15	46.23 ± 0.56	28.23 ± 3.97	18.00 ± 3.99
18	1.44 ± 0.02	0.45 ± 0.01	0.72 ± 0.01	45 ± 0.60	3.55 ± 0.03	46.28 ± 0.63	27.15 ± 1.37	19.13 ± 1.09
19	1.43 ± 0.03	0.41 ± 0.00	0.64 ± 0.00	49 ± 0.58	3.14 ± 0.01	46.40 ± 1.49	25.78 ± 1.40	20.63 ± 2.85
20	1.42 ± 0.03	0.37 ± 0.01	0.55 ± 0.00	57 ± 1.39	2.81 ± 0.04	45.38 ± 0.73	25.10 ± 25.20	20.53 ± 1.42
21	1.40 ± 0.03	0.32 ± 0.00	0.47 ± 0.00	62 ± 4.20	2.53 ± 0.08	46.90 ± 2.19	28.18 ± 2.70	18.73 ± 4.30

TABLE 6
Ranges of Measured Responses for Screening Experiments

Responses		Batch Number 1	3	4	5	6
Roll gap (in.)	Low	0.022	0.047	0.042	0.048	0.023
	High	0.168	0.204	0.216	0.207	0.201
NIR slope × 1,000	Low	0.214	0.236	0.263	0.274	0.269
	High	0.249	0.299	0.326	0.335	0.356
Meas. Rib. Dens (g/cm^3)	Low	0.592	0.731	1.006	0.936	1.009
	High	0.868	0.959	1.183	1.197	1.151
Granule mean particle size (mm)	Low	0.191	0.208	0.254	0.257	0.297
	High	0.300	0.295	0.416	0.337	0.389
Particle size increase (%)	Low	170.9	44.5	51.3	164.1	199.1
	High	325.0	105.5	148.0	214.9	260.5
Carr's index	Low	27.069	24.456	25.378	21.409	24.679
	High	34.911	28.911	30.129	30.958	32.776
Tablet tensile strength (MPa)	Low	3.815	3.277	2.386	1.129	0.970
	High	4.959	4.474	2.636	1.300	1.264

TABLE 7
Summary of Factors and Results for Batch 3

Label	Roll Gap	VFS	MS	RS	HFS	RP	NIR Slope	Rib_Dens (NIR)	Rib_Dens (Meas)	GMPS	G/RM_PS	Carr Index	RM_TTS
3–1	0.112	225	150	12	40	400	0.261	0.823	0.882	0.251	1.75	28.1	3.62
3–2	0.188	225	150	9	20	300	0.240	0.733	0.746	0.208	1.47	28.4	4.35
3–3	0.204	225	150	9	60	300	0.236	0.716	0.760	0.214	1.49	28.1	4.47
3–4	0.155	225	150	9	20	500	0.276	0.885	0.911	0.278	1.93	27.6	3.51
3–5	0.19	225	150	9	60	500	0.273	0.874	0.866	0.269	1.87	28.2	3.70
3–6	0.096	225	150	15	20	300	0.254	0.791	0.731	0.208	1.44	28.9	4.34
3–7	0.117	225	150	15	60	300	0.257	0.807	0.799	0.214	1.49	28.4	4.13
3–8	0.047	225	150	15	20	500	0.299	0.983	0.927	0.295	2.06	28.0	3.30
3–9	0.076	225	150	15	60	500	0.296	0.970	0.959	0.282	1.96	24.5	3.28

G/RM_PS, ratio of particle sizes between granule and raw material; GMPS, granule mean particle size; MS, milling speed (rpm); Rib_Dens (Meas), measured ribbon density; Rib_Dens (NIR), ribbon density determined by NIR; RM_TTS, raw material tablet tensile strength (MPa); RP, roll pressure (psi); VFS, vertical feed screw speed (rpm).

points and center replicates were added to the initial design. Preliminary experimental results showed that roll pressure was a key factor in determining ribbon and granule properties. Roll speed and HFS were crucial to roll gap but had minimal effects on this set of ribbon and granule properties. The first point of concern in a new design was that the roll gap had to be within the specification range of the compactor. This was because some difficulties were encountered in the compaction of anhydrous lactose at a high HFS speed of 65 rpm and a low roll speed of 8 rpm. Under these operating conditions, over-feeding of the roller compactor resulted in the jamming of the rolls and the VFS. To circumvent this problem, the low and high levels of the HFS speed were modified to 40 and 60 rpm, respectively, instead of 35 and 65 rpm. This change was applied to batches 12–16 (using lactose anhydrous DT and MCC Emcocel 90M SCG), as well as batches 17–21 (using lactose DMV monohydrate 200M and MCC Emcocel 50M). The difference in the ranges of HFS speed used in the preparation of batches 7–11 and 12–21 implied that the parameter spaces explored in the two cases are not identical. However, as they overlap

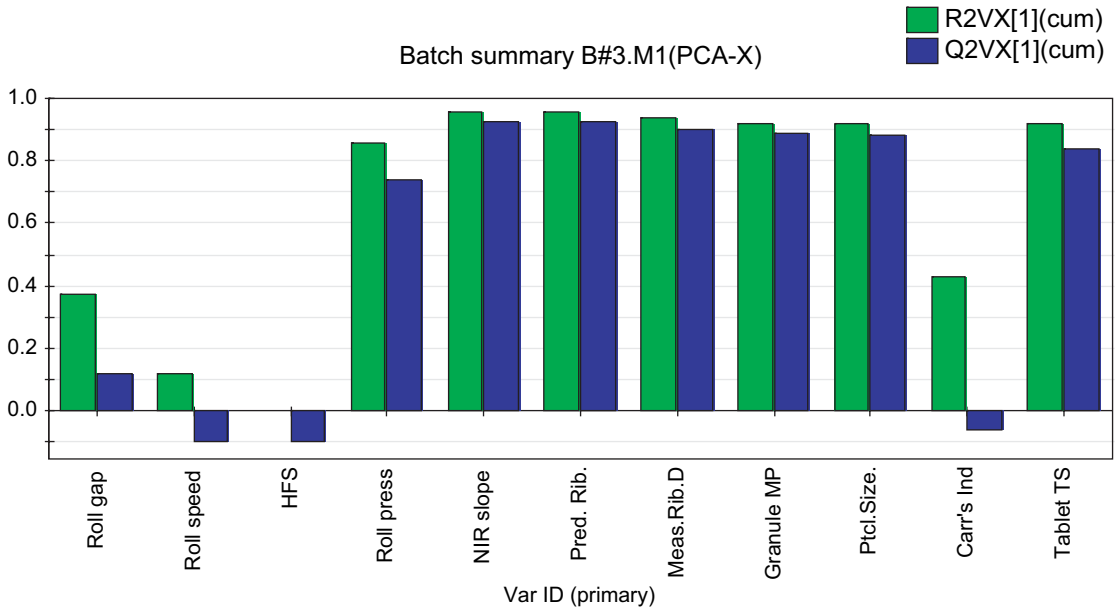

FIGURE 3. Individual R^2 and Q^2 values for the responses obtained in batch 3 using principal component analysis (PCA).

considerably, the difference between these two parameter spaces could be regarded as insignificant and would not likely affect the analysis dramatically.

PLS analysis results to predict the *Y*-variables (RC responses) using only the three OPs (roll speed, roll pressure, and HFS speed) yielded very poor model predictability (Q^2 (cum) = 0.147). Similar to the analysis results for the screening experiments earlier, roll speed exerted a strong negative effect on roll gap (Figure 5A) and a moderate negative effect on ribbon density. On the contrary, NIR slope, GMPS, and ribbon density were considerably governed by the roll pressure. High roll pressures tended to give high NIR slopes, larger granules, and denser ribbons (Figure 5A). The VIP plot in Figure 5B shows that the HFS speed was a comparatively less important OP to vary and control.

RC OPs alone fail to predict the measured responses adequately with the exception of roll gap that was significantly governed by roll speed. This was not surprising as ribbon and granule quality are largely dependent on the properties of the materials used for compaction. Hence, it was necessary to include raw material properties in the data set and evaluate changes in modeling efficiency.

Goodness of fit (R^2X = 0.897, Q^2 = 0.72) and model predictability were markedly improved when all the 16 raw material properties determined for batches 7–21 were combined with the three OPs for modeling. This model was built with six PLS components. From the coefficient overview plot (Figure 6A), it is observed that the NIR slope, GMPS, and ribbon density were well predicted by the roll pressure although GPMS was also strongly influenced by the powder flow properties (angles of repose and fall). Particle size increase from raw material to granule (G/RM_PS) was influenced by the roll gap, the kawakita constant, 1/*b*, and the powder flow parameters.

The relative importance of each *X*-variable in predicting the RC-measured responses was ranked in Figure 6B. Amongst the raw material attributes, the raw material tablet tensile strength (RM_TTS) that reflects the tabletability of the material, MCC fraction, tapped density, kawakita constant 1/*b*, and angle of fall and span were found to exert dominant effects on the various RC responses. Though the extent of interaction between the respective *X*-variables and the measured responses differed, it was evident that raw material properties contributed considerably to the robustness and prediction ability of the models built.

CONCLUSIONS

Physical characterization of the raw materials and powder blends used in the preparation of ribbons for this RC study was carried out and sixteen different material properties were determined. Differences were observed between the compressibility and the flow properties of different MCC and lactose grades. The experimental matrix for RC was stipulated in the 2^3 full factorial design with two extra axial points and two replicates of the center point to evaluate the effects of RC OPs on ribbon and granule responses. However, RC OPs alone were not able to predict ribbon and granule responses adequately. With the inclusion of raw material properties in the data set, the model predictability and goodness of fit were markedly improved. Amongst the raw material attributes, the raw material tablet

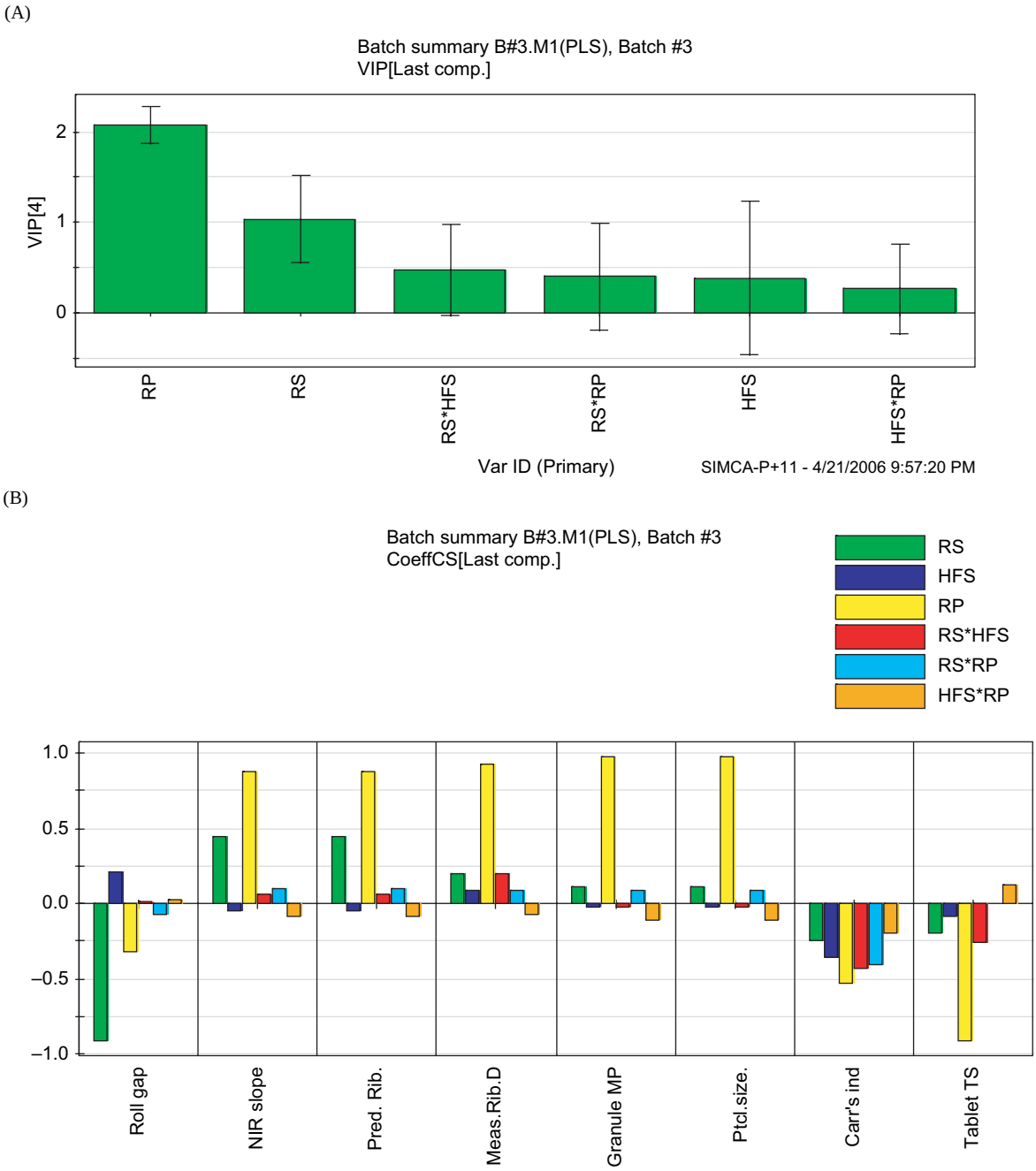

FIGURE 4. (A) Variable importance plot (VIP) and (B) coefficient overview plot for the partial least squares (PLS) regression results of batch 3.

tensile strength (RM_TTS) that reflects the tabletability of the material, MCC fraction, tapped density, kawakita constant 1/*b*, and angle of fall and span were found to exert dominant effects on the various RC responses. This study has successfully utilized a multivariate analysis method to establish the impact of raw material properties and to identify the important raw material properties that significantly affect RC responses. These preliminary findings set the foundation for later work that will examine the effects of individual raw material properties to identify critical material attributes and process critical control parameters for the implementation of a "quality-by-design" framework for RC.

ACKNOWLEDGMENTS

The authors thank the Consortium for the Advancement of Manufacturing of Pharmaceuticals (CAMP) for the funding of

(A)

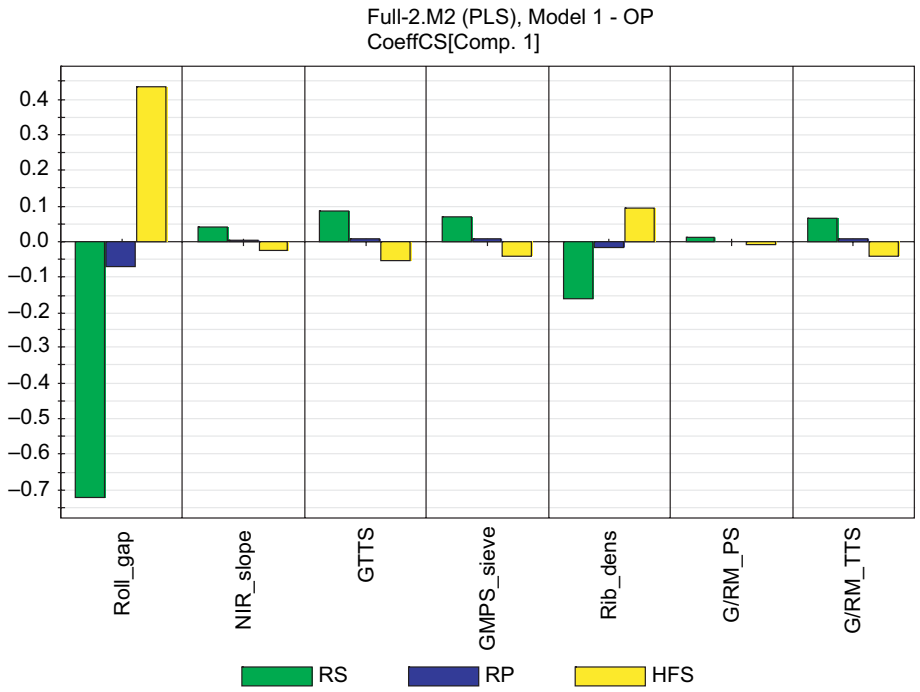

(B)

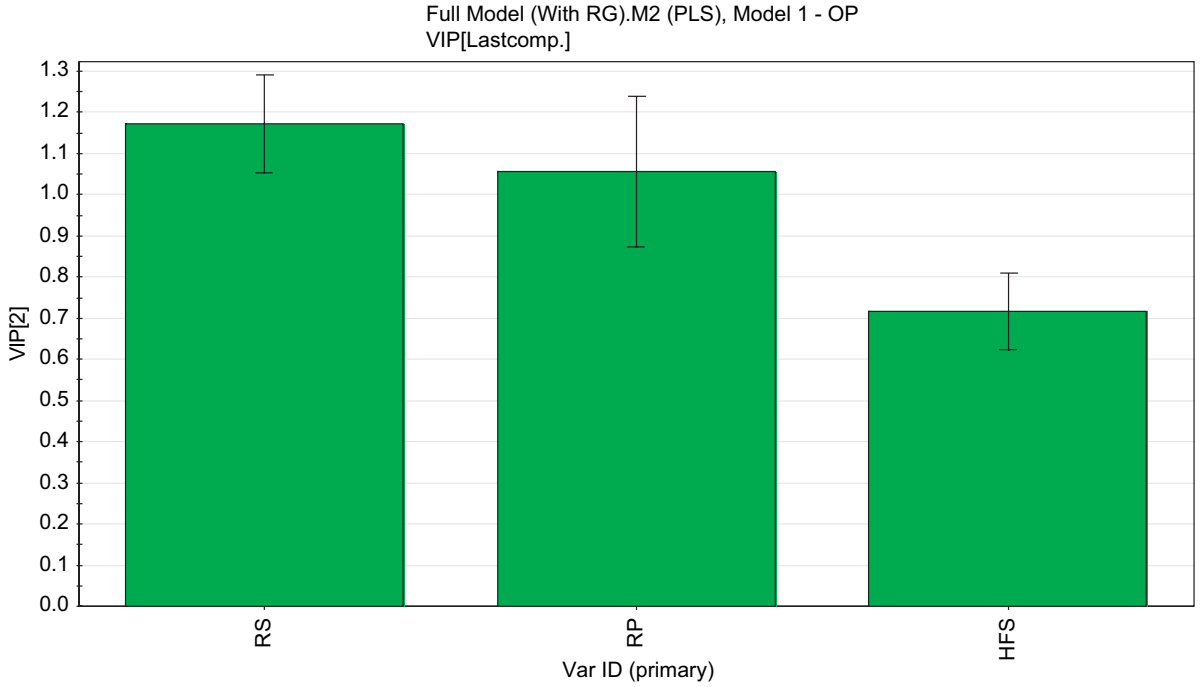

FIGURE 5. (A) Coefficient overview plot and (B) variable importance plot for partial least squares (PLS) regression results of modeling operating parameters only.

(A)

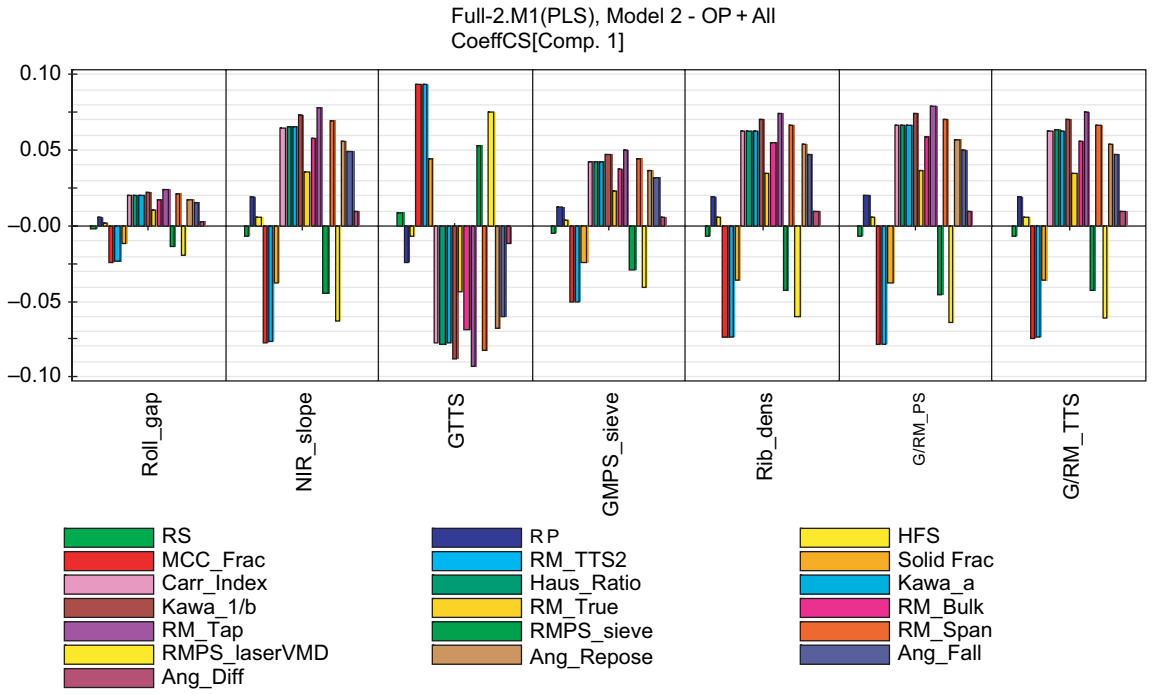

(B)

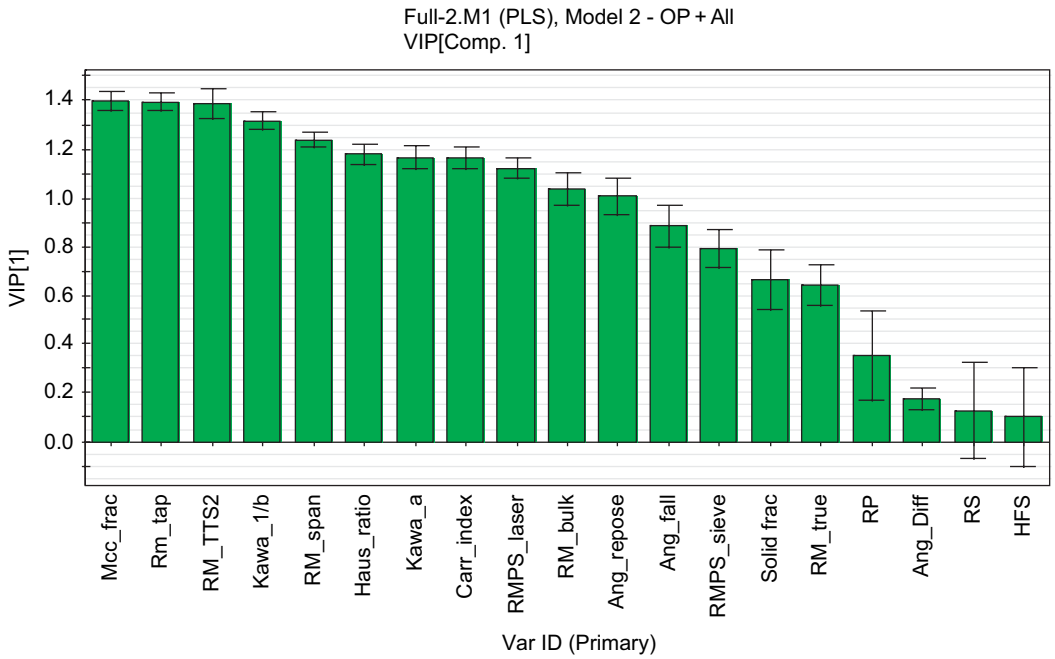

FIGURE 6. (A) Coefficient overview plot and (B) variable importance plot for partial least squares (PLS) regression results of modeling operating parameters and all the raw material properties.

this work, especially Novartis Pharmaceuticals Corporation for providing the facilities where the RC work was performed. Students from the Massachusetts Institute of Technology (MIT) Practice School are acknowledged for their help in the RC. The assistance of Victor Hildebrand in the characterization work is also appreciated.

REFERENCES

Carr, R. L. (1965). Evaluating flow properties of solids. *Chem. Eng., 72*, 163–168.

Cohn, R., Heilig H., & Delorimier A. (1966). Critical evaluation of the compactor. *J. Pharm. Sci., 55*(3), 328–331.

Dec, R. T., Zavaliangos, A., & Cunningham, J. C. (2003). Comparison of various modeling methods for analysis of powder compaction in roller press. *Powder Tech., 130*(1–3), 265–271.

Gupta, A. P. G., Miller, R. W., & Morris, K. R. (2004). Nondestructive measurements of the compact strength and the particle-size distribution after milling of roller compacted powders by near-infrared spectroscopy. *J. Pharm. Sci., 93*(4), 1047–1053.

Gupta, A. P. G., Miller, R. W., & Morris, K. R. (2005a). Real-time near-infrared monitoring of content uniformity, moisture content, compact density, tensile strength, and young's modulus of roller compacted powder blends. *J. Pharm. Sci., 94*(7), 1589–1597.

Gupta, A. P. G., Miller, R. W., & Morris, K. R. (2005b). Influence of ambient moisture on the compaction behavior of microcrystalline cellulose powder undergoing uni-axial compression and roller-compaction: A comparative study using near-infrared spectroscopy. *J. Pharm. Sci., 94*(10), 2301–2313.

Gupta, A. P. G., Miller, R. W., & Morris, K. R. (2005c). Effect of the variation in the ambient moisture on the compaction behavior of powder undergoing roller-compaction and on the characteristics of tablets produced from the post-milled granules. *J. Pharm. Sci., 94*(10), 2314–2326.

Hariharan, M., Wowchuk, C., Nkansah, P., & Gupta, V. K. (2004). Effect of formulation composition on the properties of controlled release tablets prepared by roller compaction. *Drug Dev. Ind. Pharm., 30*(6), 565–572.

Hausner, H. H. (1967). Friction conditions in a mass of metal powder. *Int. J. Powder Metall., 3*, 7–13.

Inghelbrecht, S., & Remon, J. P. (1998a). Roller compaction and tableting of microcrystalline cellulose drug mixtures. *Int. J. Pharm., 161*(2), 215–224.

Inghelbrecht, S., & Remon, J. P. (1998b). Reducing dust and improving granule and tablet quality in the roller compaction process. *Int. J. Pharm., 171*(2), 195–206.

Johanson, J. R. (1965). A rolling theory for granular solids. *J. Appl. Mech., 32*, 842–848.

Ludde, K. H., & Kawakita, K. (1967). Die pulverkompression. *Pharmazie, 21*, 93–403.

Simon, O., & Guigon, P. (2003). Correlation between powder-packing properties and roll press compact heterogeneity. *Powder Tech., 130*, 257–264.

Turkoglu, M., Aydin, I., Murray, M., & Sakr, A. (1999). Modeling of a roller-compaction process using neural networks and genetic algorithms. *Eur. J. Pharm. Biopharm., 48*(3), 239–245.